MINIMIZING THROTTLING LOSSES IN THE REFRIGERATION CYCLE

Piotr A. Domanski
National Institute of Standards and Technology
Building Environment Division
Gaithersburg, MD, U.S.A.

INTRODUCTION

Most alternative non-CFC refrigerants have a large molecular structure and large heat capacity, which influence the slope of saturated liquid line and result in substantial throttling losses in a basic reversed Rankine cycle. These losses degrade the cycle efficiency below that of the original CFC fluids; virtually all carbon-based non-hydrocarbon refrigerants have a lower Coefficient of Performance than the fluids banned by the Montreal Protocol.

This study analyzes the performance of pure-component refrigerants in the basic refrigeration (reversed Rankine) cycle and in three modified cycles in which the throttling-process irreversibilities are minimized: the liquid-line/suction-line heat exchange (lisl-hx) cycle, the economizer cycle, and the ejector cycle. The refrigerants considered in this study were the 38 fluids covered by REFPROP /1/, and REFPROP property routines were employed in performance simulations. The Carnahan-Starling-DeSantis equation of state was applied for all fluids except ammonia, for which a formulation by Harr and Gallagher was used.

THROTTLING LOSSES

Thermodynamically, all refrigerants have the same COP potential in the ideal vapor compression cycle*. At prescribed condenser and evaporator temperatures, this potential is defined by the Coefficient of Performance of the reversed Carnot refrigeration cycle,

$$COP_C = \frac{T_{evap}}{T_{cond} - T_{evap}}$$

Since the Carnot cycle is completely reversible, it is an unattainable ideal model for a refrigeration cycle. Consequently, the more realistic Rankine cycle is used to represent the thermodynamic processes in a refrigeration machine. Both cycles are shown in Figure 1. The work for the Rankine cycle includes that for the Carnot cycle plus the work depicted by the triangle 2_C-2-2_V and the rectangle located under the line 4_C-4_R. The first area represents the additional work required due to vapor superheating above the temperature of the heat sink, while the second corresponds to the work needed to compensate for the irreversible expansion

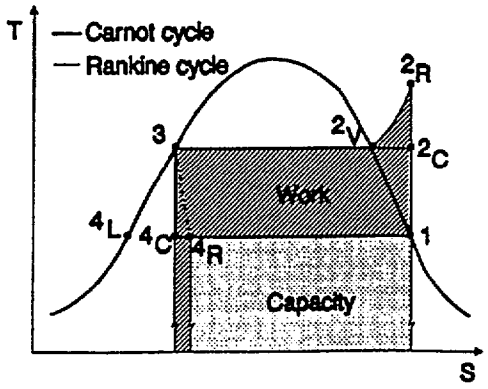

Figure 1. Carnot and Rankine cycle (Work and capacity marked for the Rankine cycle)

* This discussion is given here for completeness although it can be found elsewhere.

process $3\text{-}4_R$. The area under the line $4_C\text{-}4_R$ also represents the loss of refrigerating capacity.

Based on these observations from Figure 1, we can write the following equation for COP_R:

$$COP_R = \frac{Q_R}{W_R} = COP_C \frac{1 - \frac{Q_{exp}}{Q_C}}{1 + \frac{W_{exp}}{W_C} + \frac{W_{sup}}{W_C}}$$

Using a few simplifying assumptions, we can express Q_{exp}/Q_C by the following equation /2/:

$$\frac{Q_{exp}}{Q_C} = \frac{\frac{1}{COP_C} - \ln\frac{T_{cond}}{T_{evap}}}{\frac{h_{fg}}{T_{evap}\,\bar{c}_{p,l}} - \ln\frac{T_{cond}}{T_{evap}}}$$

The relative loss of work due to isentropic expansion, W_{exp}/W_C, is related to Q_{exp}/Q_C through the Carnot efficiency, $W_{exp}/W_C = COP_C \cdot Q_{exp}/Q_C$, since $W_{exp} = Q_{exp}$ and $W_C = Q_C/COP_C$.

Only one term in the derived relation for Q_{exp}/Q_C is fluid-property dependent, while the remaining three terms depend on operating conditions. If we evaluate refrigerants at the same absolute or reduced temperatures in the evaporator and condenser, the relative loss of the refrigerating capacity will depend solely on the latent heat, heat capacity of liquid at constant pressure, and the absolute temperature in the evaporator.

The penalties degrading the Rankine cycle COP_R relative to the Carnot cycle, Q_{exp}/Q_C, W_{exp}/W_C, and W_{sup}/W_C, are presented in Figure 2. For simplicity, these penalties are graphed on one bar for each fluid, though they do not have a straight additive effect on the COP. Fluids of large heat capacity do not have superheated-horn losses (compression process ends in the wet-vapor region), but they have the largest total losses due to throttling. Overall, the penalties caused by the isenthalpic expansion constitute the largest part of the total losses in the theoretical cycle.

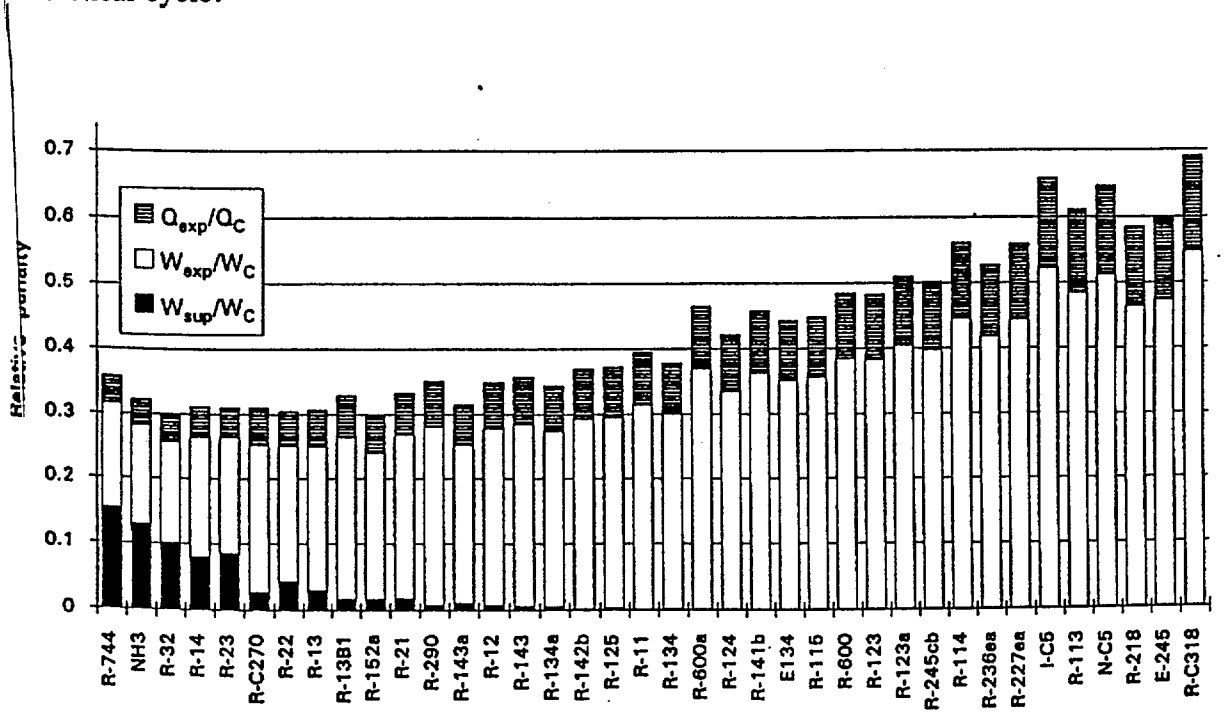

Figure 2. Relative penalties degrading the Rankine cycle COP ($T_{evap,r}$=0.65, $T_{cond,r}$=0.82, refrigerants sorted by $c_{p,v}$ at T_r=0.65)

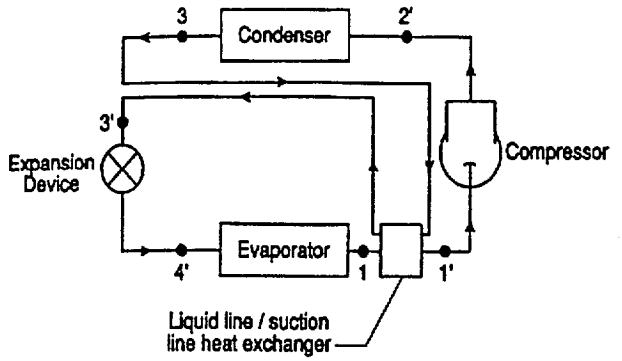

Figure 3. Schematic for llsl-hx cycle

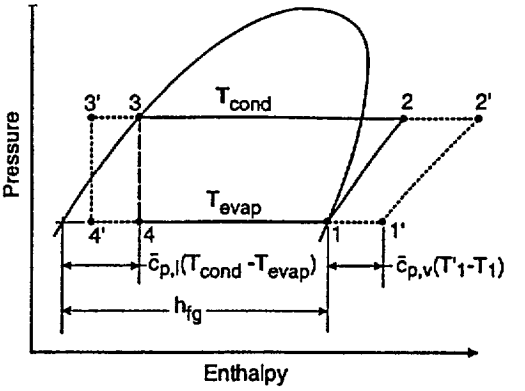

Figure 4. P-h diagram for llsl-hx cycle

The cycle simulations in this study were performed at the evaporator and condenser reduce temperatures of $T_{evap,r}=0.65$ and $T_{cond,r}=0.82$. This allowed examining a diverse set o refrigerants at their best operating temperature range while still testing them against the sam COP limit of the Carnot cycle. The results are presented for refrigerants sorted by $c_{p,v}$ becaus at the same reduced temperature $c_{p,v}$ and $c_{p,l} \cdot T/h_{fg}$ for different fluids are almost linearl related. Simulations at specified absolute temperatures are included in the source report /2/

CYCLE WITH LIQUID-LINE/SUCTION-LINE HEAT EXCHANGER

In the llsl-hx cycle, a heat exchanger is installed to subcool the high-pressure refrigerant wit the low-pressure suction vapor, which is being superheated in the process. Figure 3 shows th schematic of this cycle. Figure 4 presents the basic and llsl-hx cycle on the P-h diagram. Th pertinent publications on llsl-hx cycle are included in reference /3/.

Subject to a few simplifying assumptions, the factors affecting COP_{hx} are shown in th following equation /3/:

$$\frac{COP_{hx}}{COP_R} = \frac{\frac{Q_{hx}}{Q_R}}{\frac{W_{hx}}{W_R}} = \frac{1 + \dfrac{T_1' - T_1}{h_{fg}/\bar{c}_{p,v} - (T_{cond} - T_{evap})\,\bar{c}_{p,l}/\bar{c}_{p,v}}}{1 + \beta_v \cdot (T_1' - T_1)}$$

Addition of the liquid-line/suction-line heat exchanger to the Rankine cycle affects both cycl capacity and work and may have positive or negative performance implications. Figure 5 presents the capacity and work for the theoretical limit of 100% effectiveness of the llsl-hx related to those of the Rankine cycle. The figure shows that the change in work required doe not vary significantly between different fluids, but the change in capacity varies considerably with the molar heat capacity of vapor.

Figure 6 presents the coefficient of performance of the llsl-hx cycle, COP_{hx}, referenced to the COP of the Carnot cycle for three values of the llsl-hx effectiveness ($\eta_{hx}=0$. constitutes the Rankine cycle). The figure shows that fluids of low molar heat capacity do not benefit from the installation of the llsl-hx, and perform better in the basic, unmodified Rankine cycle. For the fluids of very low heat capacity, the COP declines when the llsl-hx is installed. Fluids of a high molar heat capacity have a low COP in the Rankine cycle, but their performance improves with llsl heat exchange and can exceed the COP of the best performing fluids in the Rankine cycle at the theoretical limit of 100% effectiveness of the llsl-hx.

The COP improvement potential due to installation of the llsl-hx may be hampered by refrigerant pressure drop on the vapor side of llsl-hx. Simulations for R-115 and R-123 a $T_{evap,r}=0.65$ and $T_{cond,r}=0.82$ showed that 20 kPa pressure drop totally eliminates the COP benefit of the 50% effective heat exchanger. Refrigerant pressure drop on the liquid-line side of llsl-hx showed no effect on the cycle performance.

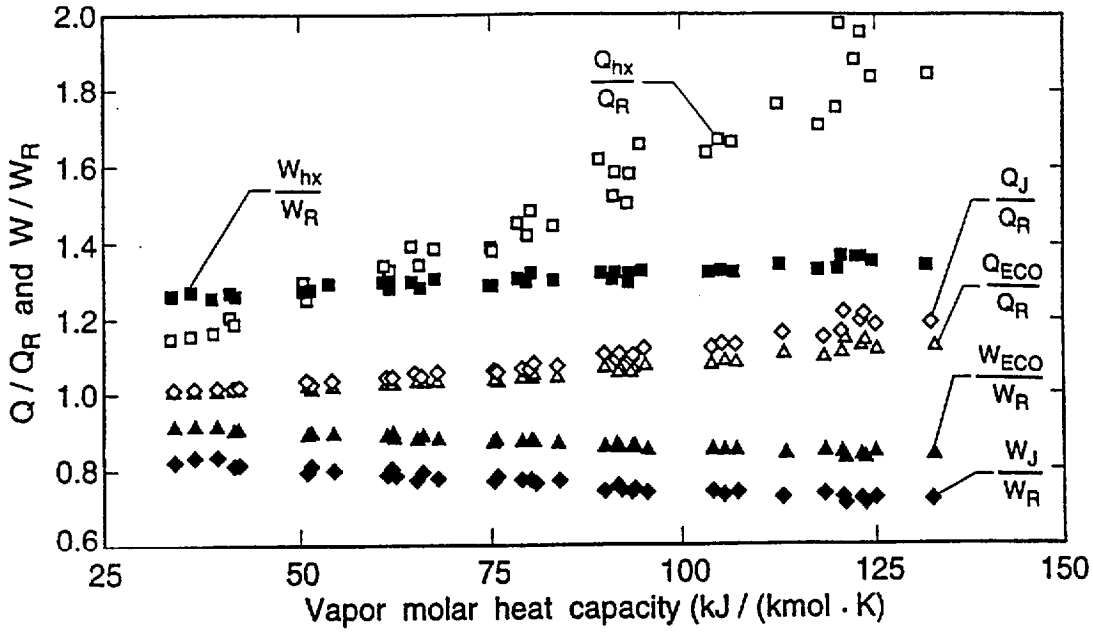

Figure 5. Capacity and work of the modified cycles referenced to capacity and work of the Rankine cycle ($T_{evap,r}$=0.65, $T_{cond,r}$=0.82, η_{hx}=100%, eff=100%)

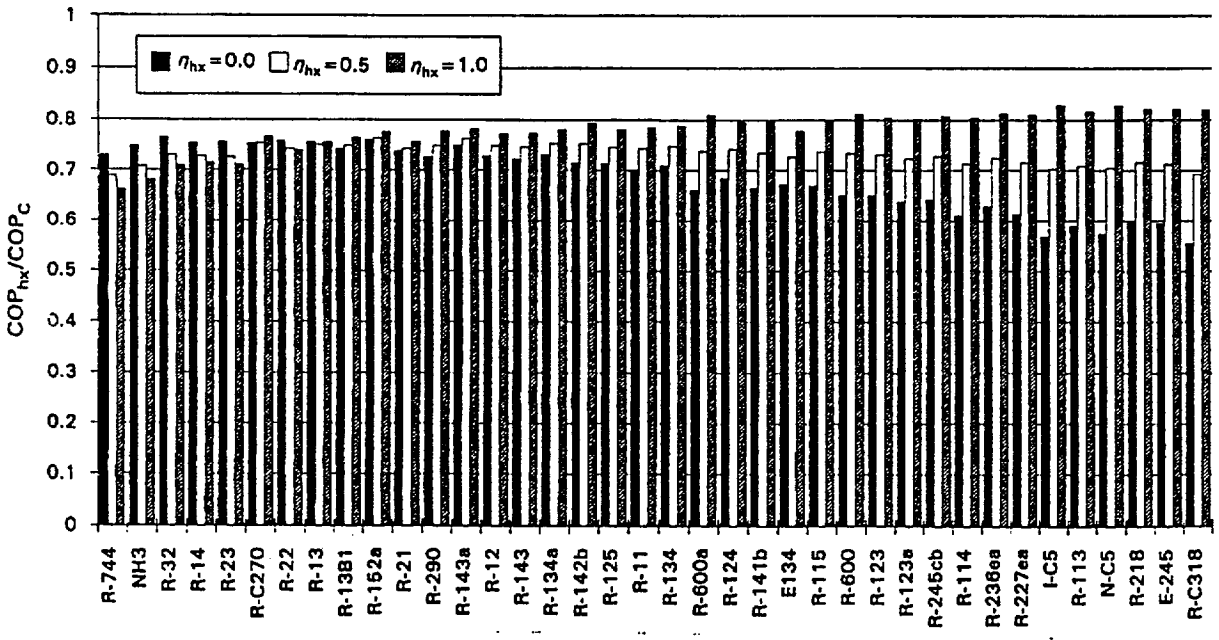

Figure 6. COP of the IIsI-hx cycle referenced to COP_C ($T_{evap,r}$=0.65, $T_{cond,r}$=0.82)

ECONOMIZER CYCLE

The economizer refrigeration cycle differs from the Rankine cycle by a two-stage expansion with a liquid/vapor separator, and a compressor equipped with an intermediate-pressure suction port. In the economizer cycle (shown in Figures 8 and 9), the liquid and vapor phases are separated after the first-stage expansion; the vapor is fed to the intermediate stage of the compressor, and the liquid undergoes further expansion on its way to the evaporator.

Figure 5 includes the capacity and work of the economizer cycle referenced to the respective values of the Rankine cycle. The economizer cycle improves the COP for each fluid since changes in both capacity and work promote an improvement of the system COP_{ECO}. Figure 9 displays the ratios of COP_{ECO} and COP_R to COP_C. The COPs of different refrigerants are more uniform for the economizer cycle than for the Rankine cycle. The best-performing fluids in the Rankine cycle are still the best performers in the economizer cycle.

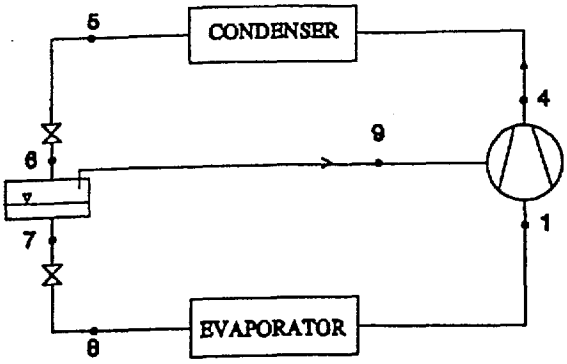

Figure 7. Schematic of economizer cycle

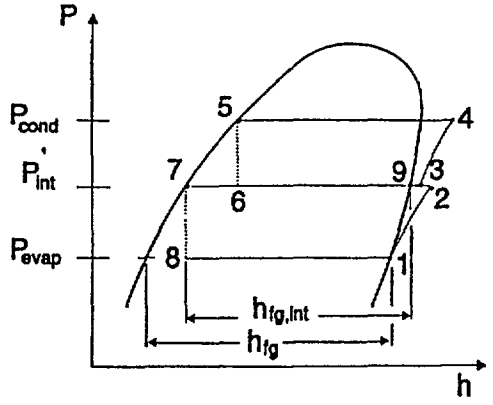

Figure 8. P-h diagram for economizer cycle

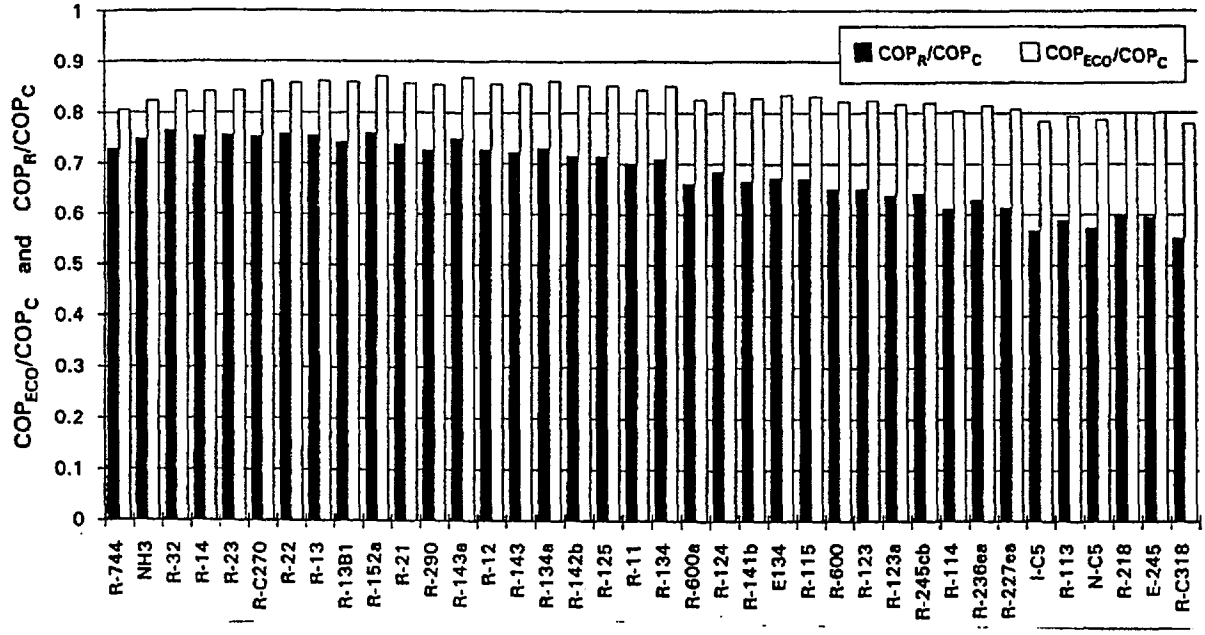

Figure 9. COP of the economizer cycle and cycle referenced to COP_C ($T_{evap,r}$=0.65, $T_{cond,r}$=0.82)

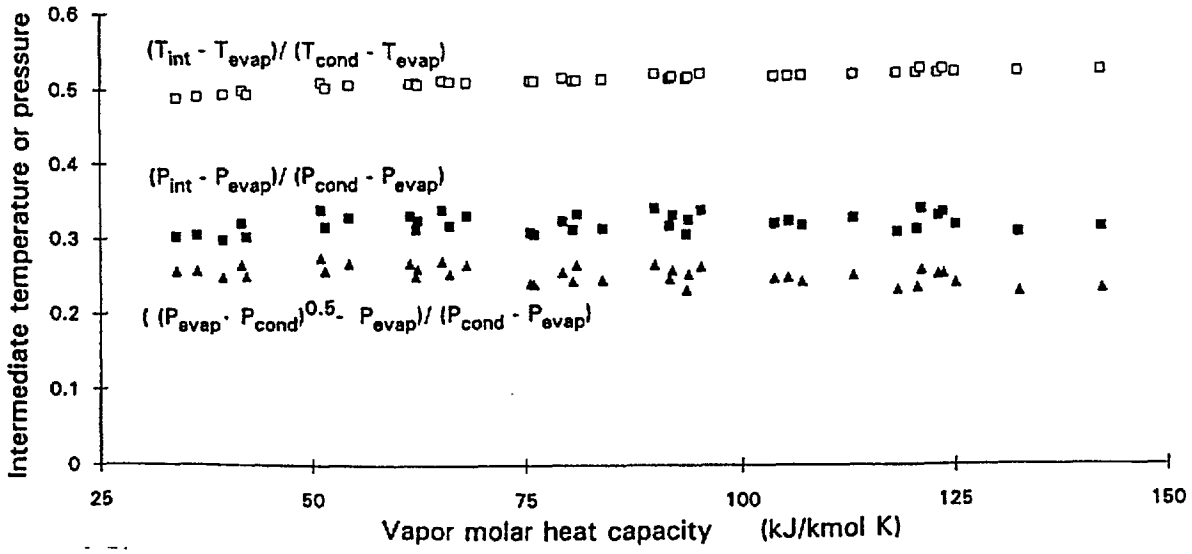

Figure 10. Optimum intermediate temperature, pressure, and geometric-mean intermediate pressure ($T_{evap,r}$=0.65, $T_{cond,r}$=0.82)

The optimum intermediate saturation temperature, T_{int}, is fairly uniform for the fluids considered and can be well approximated by the mean temperature between the condenser and evaporator (i.e., $0.5(T_{cond}+T_{evap})$). There is some dependency of the optimum T_{int} on molar heat capacity, but it is rather small, as shown in Figure 10. The optimum pressure is also uniform, but correlates with more scatter. The geometric mean pressure (i.e.,$(P_{cond} \cdot P_{evap})^{0.5}$), which ensures the minimum work for two-stage compression of a perfect gas with complete intercooling /4/, underestimates the optimum pressure for the real gases in the economizer cycle. The mean temperature also indicates the optimum intermediate temperature well for other combinations of evaporator and condenser temperatures.

EJECTOR CYCLE

The majority of work in ejectors has been for single-phase applications. An extensive list of publications on the topic is given in /5/. In the application considered here, the ejector is employed to reduce throttling irreversibilities through the use of kinetic energy of flash gas to increase refrigerant suction pressure at the compressor inlet. Besides basic system components, the cycle includes a jet ejector and separator, which are configured in the system as shown in Figure 11. The ejector itself consists of four main parts: the motive (primary) nozzle, suction nozzle, mixing section, and diffuser. High-pressure refrigerant expands and accelerates in the motive nozzle and mixes with the refrigerant vapor which enters the ejector through the suction nozzle. The mixture decelerates in the diffuser which increases mixture pressure above the pressure in the evaporator. The separator separates the two-phase stream into saturated vapor and liquid. The vapor enters the compressor while the liquid is directed to the evaporator through a small-pressure-drop expansion device. Since the compression process starts from a higher pressure than the evaporator pressure, compression work is reduced. Also, withdrawal of energy from the expanding refrigerant results in a lower refrigerant quality entering the evaporator. The resulting effect is an increase in the cycle COP and volumetric capacity.

The analysis of the ejector followed the assumptions and calculating scheme presented by Kornhauser /6/ for one-dimensional simulation of the ejector. Properties and velocities of the refrigerant were assumed to be uniform over any cross section. The streams entering and leaving the ejector were at stagnation conditions, and the mixing of the motive fluid and secondary vapor took place at constant pressure. The processes in the motive and suction nozzles were represented by their respective efficiencies, so that velocities at the outlets could be calculated as follows:

The motive nozzle: $u_m = \sqrt{2(h_{m,i} - h_{m,o})}$ $\qquad h_{m,o} = h_{m,i} - \eta_m(h_{m,i} - h_{m,o,is})$

The suction nozzle: $u_s = \sqrt{2(h_{s,i} - h_{s,o})}$ $\qquad h_{s,o} = h_{s,i} - \eta_s(h_{s,i} - h_{s,o,is})$

where the enthalpies following the isentropic expansion, $h_{m,o,is}$ and $h_{s,o,is}$, were defined by the respective inlet entropies to the nozzles and pressure in the mixing section.

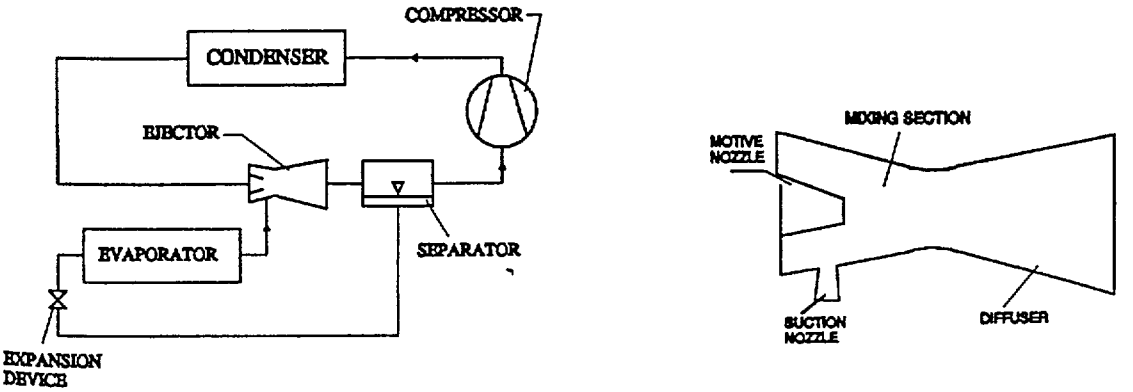

Figure 11. Schematic of the ejector system

Conservation of mass, momentum, and energy for the mixing process results in:

$$r_m + r_s = 1$$

$$u_x = u_m r_m + u_s r_s$$

$$h_x = h_{m,i} \cdot r_m + h_{s,i} \cdot r_s - \frac{u_x^2}{2}$$

Refrigerant enthalpy at the diffuser outlet, h_d, was calculated by the equation: $h_d = h_x + u_x^2/2$. The pressure at the diffuser outlet, $P_d = f(h_d', s_x)$, was calculated applying the diffuser efficiency concept and the energy conservation equation, $h_d' = h_m + \eta_d \cdot u_m^2/2$, where s_x is refrigerant entropy after the mixing process defined by h_x and P_x.

The ejector cycle COP is affected by the individual efficiencies of the motive nozzle, suction nozzle, and diffuser /6/ and the mixing pressure in the ejector. In all simulations performed for this study, the mixing pressure was optimized for each fluid to provide maximum COP. As shown in Figure 5, the ejector cycle realizes an improvement in both the capacity and work requirement. The trend of Q_j/Q_r and W_j/W_r is very similar to that for the economizer cycle, but the benefit displayed for the ejector cycle (which presents the results for all ejector component efficiencies equal to 100%) is greater. However, if the ejector component efficiencies were all lowered to 80%, the results would be nearly identical to the economizer cycle.

Figure 12 presents the COP of the ejector cycle for different levels of ejector component efficiency. The lowest bars in the figure are for a system with the ejector efficiency equal to zero, which reduces the ejector cycle to the Rankine cycle. The additional bar fragments indicate COPs for different levels of ejector component efficiency. At low ejector component efficiencies, low heat capacity refrigerants have a better COP. At high ejector component efficiencies, high heat capacity fluids show a higher COP.

The simulations presented above included high efficiencies of the ejector components, which may not be attainable in practice. It is safe to assume that the efficiencies attainable in a single-phase system (0.85-0.9 for a nozzle and 0.7 for a diffuser) are the practical limits for two-phase ejectors. With very limited research done so far on two-phase ejector, it is unknown to what degree they can approach the performance level of the single-phase devices.

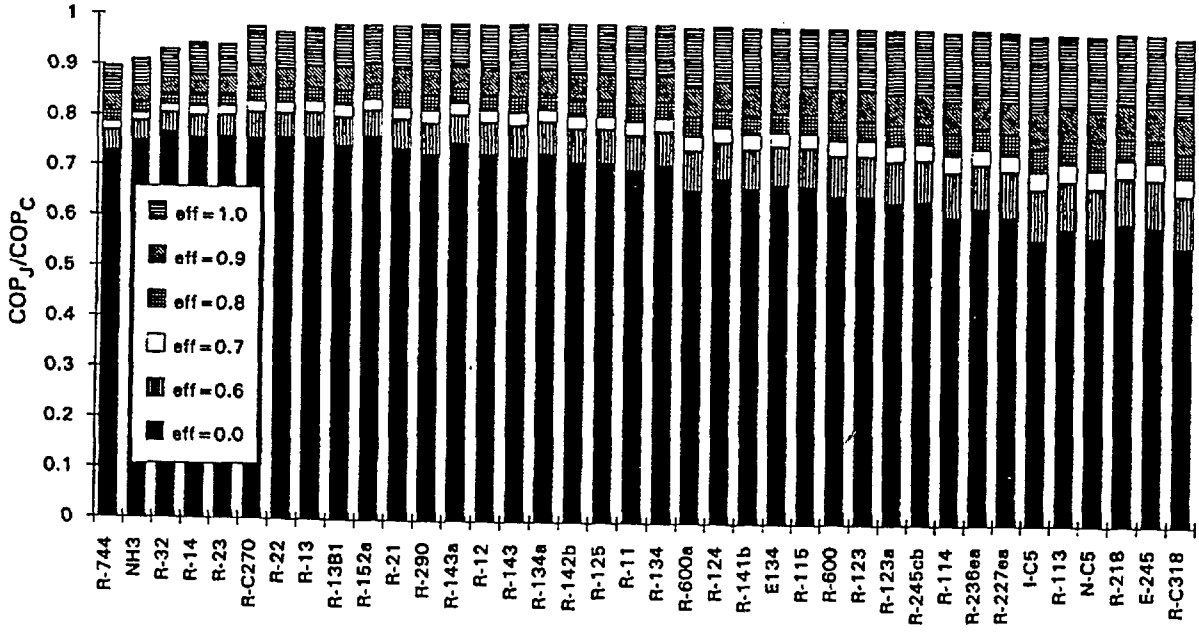

Figure 12. COP of the ejector cycle referenced to COP_C ($T_{evap,r}$=0.65, $T_{cond,r}$=0.82)

SUMMARY

At given reduced temperatures in the evaporator and condenser, the molar heat capacity is the dominating factor determining the throttling losses. The capability to improve the system COP increases with the amount of throttling losses for all three modified cycles. Between the three options considered, the cycle with liquid-line/suction-line heat exchange showed the smallest COP improvement potential. While the llsl-hx improves the COP of large molar heat capacity refrigerants which have a low COP_R, it may penalize the COP of refrigerants with small molar heat capacity, which have the highest COP_R. The economizer and ejector cycle increase the COP for all fluids. The improvement results from both the increased capacity and reduced work, the latter having a more significant effect.

The COP of the ejector cycle is very sensitive to the ejector efficiency. Because of limited knowledge of two-phase ejectors, it is unclear what efficiency level they can achieve. When the single-phase component efficiencies (0.85 for a nozzle, 0.7 for a diffuser) were used in simulations for R-134a at two operating regimes (T_{evap}=-10°C, T_{cond}=46°C, and T_{evap}=8°C, T_{cond}=46°C), the economizer cycle had a marginally better COP than the ejector cycle.

NOMENCLATURE

$\underline{c_p}$ - molar heat capacity at constant pressure
$\bar{c}_p$ - average value
eff - efficiency of ejector components
h - enthalpy
r - fraction of total flow
s - entropy
T - temperature
u - velocity
v - specific volume
Q - heat, capacity
$\underline{W}$ - work
β - average value of coefficient of thermal expansion
η_{hx} - effectiveness of llsl-hx

Subscripts:

C - Carnot
cond - condenser
crit - critical
d - diffuser
ECO - economizer
evap - evaporator
exp - isenthalpic expansion
hx - llsl-hx cycle
i - inlet
int - intermediate
J - ejector
l - liquid
m - motive nozzle in ejector
o - outlet
R - Rankine
s - suction nozzle in ejector
sup - related to superheated vapor horn
r - reduced value
v - vapor
x - mixing section in ejector

REFERENCES

/1/ Gallager, J., McLinden, M., Morrison, G., and Huber, M., "NIST Thermodynamic Properties of Refrigerants and Refrigerant Mixtures Database (REFPROP)", Version 4., NIST Standard Reference Database 23, National Institute of Standards and Technology, Gaithersburg, MD, November 1993.

/2/ Domanski, P.A., Theoretical Evaluation of the Vapor compression Cycle With a Liquid-Line/Suction Line Heat Exchanger, Economizer, and Ejector, NISTIR-5606, National Institute of Standards and Technology, Gaithersburg, MD, March 1995.

/3/ Domanski, P.A., Didion, D.A., and Doyle, J.P., "Evaluation of Suction-Line/Liquid -Line Heat Exchange in the Refrigeration Cycle", Int. J. Ref., Vol. 17, No. 7, 1994.

/4/ Threlkeld, J.L., "Thermal Environmental Engineering", Prentice-Hall, Inc., Englewood Cliffs, NJ, 1970.

/5/ Huang, B.J., Jiang, C.B., and Hu, F.L., "Ejector Performance Characteristics and Design Analysis of Jet Refrigeration System", Transactions of ASME, Vol. 107, pp. 792-802, July 1985.

/6/ Kornhauser, A.A., "The Use of an Ejector as a Refrigerant Expander", Proc. ASHRAE-Purdue CFC Conference, Int. Inst. Refrig., Paris, pp. 10-19, 1990.

ACKNOWLEDGEMENT

This study was sponsored by the Advanced Technology Program at the National Institute of Standards and Technology. The author thanks P. Rothfleisch and D. Didion of NIST and P. Glamm of the Trane Company for their comments.